



# Insights into nitrogen cycling in the western Gulf of California from the nitrogen isotopic composition of diatom-bound organic matter

**Julie F. Kalansky**

*Institute of Marine and Coastal Sciences, Rutgers University, 71 Dudley Road, New Brunswick, New Jersey 08901, USA (kalansky@marine.rutgers.edu)*

**Rebecca S. Robinson**

*Graduate School of Oceanography, University of Rhode Island, South Ferry Road, Narragansett, Rhode Island 02882, USA (rebeccar@gso.uri.edu)*

**Brian N. Popp**

*Department of Geology and Geophysics, University of Hawai'i at Mānoa, 1680 East-West Road, Honolulu, Hawaii 96822, USA*

[1] The nitrogen isotopic composition of organic matter contained within diatom frustules of different sediment size fractions from the Guaymas Basin, Gulf of California, suggests that multiple nutrient cycling processes can be examined from a single sediment sample. The diatom-bound  $\delta^{15}\text{N}$  values from the greater and less than  $63\ \mu\text{m}$  size fractions were analyzed from six intervals of core MD02–2517, each representing ~30–40 years. The diatom-bound  $\delta^{15}\text{N}$  values are compared to bulk sedimentary  $\delta^{15}\text{N}$  values, weight percent biogenic opal, and weight percent organic carbon. Bulk sedimentary  $\delta^{15}\text{N}$  values range from 10‰ to 12.5‰ and diatom-bound  $\delta^{15}\text{N}$  values of the  $<63\ \mu\text{m}$  size fraction from 7‰ to 13‰. In contrast, diatom-bound  $\delta^{15}\text{N}$  values for the  $>63\ \mu\text{m}$  fraction range from 1‰ to 7‰. The best explanation for the low diatom  $\delta^{15}\text{N}$  values in the  $>63\ \mu\text{m}$  fraction is that the large diatoms grew at the base of the euphotic zone in excess nitrate and under low light conditions. Large diatom  $\delta^{15}\text{N}$  values correlate significantly with bulk sedimentary  $\delta^{15}\text{N}$  values ( $r = 0.68, 0.82$ ), indicating that large diatoms, such as *Thalassiothrix longissima*, are an important component of export production fueled by a nonupwelling source of nitrogen. The  $>63\ \mu\text{m}$  diatoms are estimated to contribute between 3% and 15% of the total nitrogen in the sediments based upon an assumed Si-to-N ratio of 1.2.

**Components:** 8100 words, 5 figures, 1 table.

**Keywords:** Gulf of California; diatoms; export flux; nitrogen cycling; nitrogen isotopes.

**Index Terms:** 0469 Biogeosciences: Nitrogen cycling; 1041 Geochemistry: Stable isotope geochemistry (0454, 4870); 4912 Paleoclimatology: Biogeochemical cycles, processes, and modeling (0412, 0414, 0793, 1615, 4805).

**Received** 15 November 2010; **Revised** 20 April 2011; **Accepted** 26 April 2011; **Published** 25 June 2011.

Kalansky, J. F., R. S. Robinson, and B. N. Popp (2011), Insights into nitrogen cycling in the western Gulf of California from the nitrogen isotopic composition of diatom-bound organic matter, *Geochem. Geophys. Geosyst.*, 12, Q06015, doi:10.1029/2010GC003437.

## 1. Introduction

### 1.1. Nitrogen Cycling in the Gulf of California

[2] Nitrogen (N) is an essential nutrient and its availability has the potential to limit biological productivity in the oceans. However, the biogeochemical cycling of N is not well constrained. Holocene isotopic records suggest that the nitrogen budget is relatively balanced [Altabet, 2007; Brandes and Devol, 2002], but modeling studies based on the Redfield ratio imply that, at present, sinks are two times greater than the sources [Codispoti, 2007; Deutsch et al., 2007]. The major sink for N is denitrification, the microbial reduction of nitrate ( $\text{NO}_3^-$ ) to  $\text{N}_2$  in the absence of oxygen. Nitrate is the most common dissolved species of bioavailable N in the ocean. The primary source of new N to the oceans is  $\text{N}_2$  fixation, the bacterial acquisition of N from  $\text{N}_2$ . Within the Gulf of California (GoC) several key N cycling processes occur, including denitrification,  $\text{N}_2$  fixation, and variable degrees of upwelling and export production. Measurements of the N isotopic composition of distinct sedimentary pools are investigated as a potential tool for studying past sources and sinks of nitrogen. The aim of the research is to improve our understanding of the N cycle and its role in driving export in the region.

[3] The major sink of bioavailable nitrogen in the GoC is denitrification. Water column denitrification in the GoC results from the influx of oxygen-poor Pacific Ocean waters [Lavín and Marinone, 2003] and local oxygen demand associated with the export of organic carbon. Nitrogen isotope fractionation associated with denitrification results in nitrate  $\delta^{15}\text{N}_{\text{nitrate}}$  values ( $\delta^{15}\text{N}_{\text{nitrate}}$ ) that are elevated by as much as 15‰ relative to the oceanic mean (~5‰) in the suboxic zones of the open Pacific [De Pol-Holz et al., 2009; Liu and Kaplan, 1989; Sigman et al., 1999]. Waters from the Pacific that enter the GoC have  $\delta^{15}\text{N}_{\text{nitrate}}$  values of ~12‰, but during the summer of 2008, the  $\delta^{15}\text{N}_{\text{nitrate}}$  was as high as 24.6‰ at 300 m in the GoC [Granger and Sigman, 2009]. The elevation of  $\delta^{15}\text{N}_{\text{nitrate}}$  values in the GoC relative to that in the eastern tropical North Pacific is indicative of the extensive contribution of local denitrification within the GoC.

[4] The sources of nitrogen to the surface waters vary seasonally as a result of bimodal weather patterns within the GoC [Thunell, 1998; White et al., 2007]. In winter, the Great Basin High, located over the southwestern United States, creates strong NW surface winds [Badan-Dangon

et al., 1991; Thunell, 1998] that induce upwelling along the mainland side of the GoC. The upwelling supports significant productivity, as reflected by the high winter chlorophyll concentrations measured by Coastal Zone Color Scanner (CZCS) [Thunell, 1998]. In summer, when a low forms over Arizona, the winds are reversed and diminished. The weaker SE winds and higher sea surface temperatures result in a highly stratified water column in the central GoC that effectively cuts off the supply of nutrients to the mixed layer in most parts of the GoC [Thunell, 1998; White et al., 2007]. The water that is upwelled prior to stratification has previously undergone partial water column denitrification. Thus, when all the nitrate is consumed excess phosphate remains in surface waters [White et al., 2007]. This excess phosphate in the strongly stratified mixed layer creates an environment conducive to  $\text{N}_2$  fixation [Deutsch et al., 2007; White et al., 2007]. Significant rates of nitrogen fixation ( $132\text{--}230 \mu\text{mol N m}^{-2} \text{d}^{-1}$ ) were documented in the GoC during the summer of 2005 and could account for 35–48% of N demand by phytoplankton in that period [White et al., 2007].

[5] Although not as well studied as the seasonal cycle of surface primary production, productivity within the deep chlorophyll maximum (DCM) is important to carbon export and nutrient cycling. The DCM may be a response to the nutrient limited surface water during the highly stratified months and contribute significantly to total productivity of the GoC. The depth of the DCM corresponds with the upper part of the nitracline ( $[\text{NO}_3^-] > 1 \mu\text{M}$ ) [Hidalgo-González and Alvarez-Borrego, 2001] and typically shoals when the mixed layer depth is deeper and/or when the water column is less stratified [Hidalgo-González and Alvarez-Borrego, 2001]. A qualitative analysis of cells during July of 2008 revealed a high abundance of diatoms at depths below 25 m, whereas in shallower depths smaller algae and heterotrophic bacteria were more dominant (R. Foster, personal communication, 2009).

### 1.2. Sedimentary Records in the GoC

[6] Core and sediment trap studies from Guaymas Basin, located within the central and western GoC, reveal an annual depositional cycle; the sediment is deposited in couplets of opal and lithogenic material (annual laminae pairs) (Figure 1) [Altabet et al., 1999; Calvert, 1966; Thunell, 1998]. Opal from diatom production dominates during the winter upwelling season. In summer, opal flux decreases and the lithogenic flux increases, resulting in the

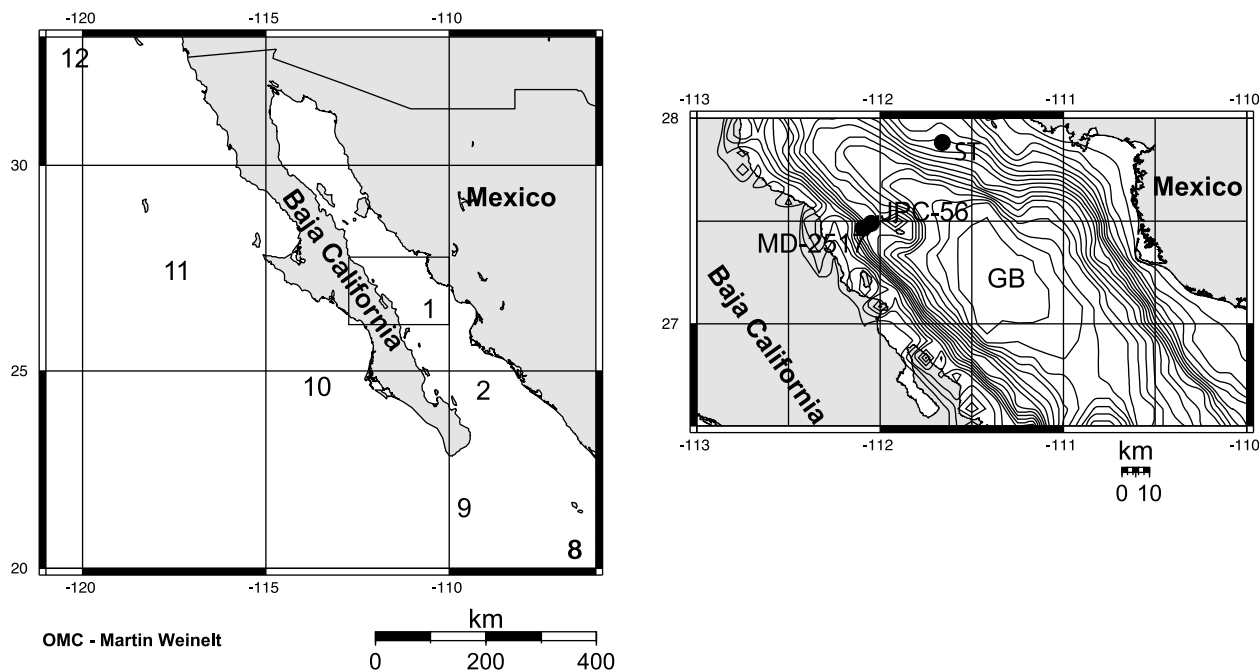


**Figure 1.** Sampling locations within and around the Gulf of California. (left) The numbers represent water column sampling stations. (right) The core location (MD-2517) with bathymetry lines showing the slopes of Guaymas Basin (GB). Black circles mark the location of the core used in this study as well as the sediment trap (ST) and the giant piston core sites (JPC-56).

darker, summer laminae [Thunell, 1998]. Analysis of cored intervals by scanning electron microscope reveals a more detailed annual cycle within the sediment (for details see Kemp *et al.* [2000]). The diatom taxa *Stephanopyxis palmeriana*, *Rhizosolenia* spp., *Thalassiothrix longissima*, and large *Coscinodiscus* spp. are all associated with the “fall dump” that occurs when the summer thermocline breaks down due to the onset of NW winds and deposits large quantities of opal from these species [Kemp *et al.*, 2000].

[7] The nitrogen isotopic composition of sediment trap material varies seasonally; particulate  $\delta^{15}\text{N}$  values ( $\delta^{15}\text{N}_{\text{PM}}$ ) are low during the winter and increase into the summer [Altabet *et al.*, 1999; Pride *et al.*, 1999]. This is attributed to the fractionation by phytoplankton during uptake and assimilation of nitrate. Diatoms and other photosynthetic organisms preferentially use  $^{14}\text{NO}_3^-$ . The remaining  $\text{NO}_3^-$  becomes progressively enriched during drawdown [Wada and Hattori, 1976]. During the summer when nutrients are limited,  $\delta^{15}\text{N}_{\text{PM}}$  values tend to be high as nutrients are used to near completion. This pattern of high  $\delta^{15}\text{N}_{\text{PM}}$  values during the summer is not observed every year. For example, during 1990 and 1991 the lowest  $\delta^{15}\text{N}_{\text{PM}}$  values were recorded in the fall

while in 1992 the lowest value was recorded in late summer [Altabet *et al.*, 1999]. The occurrence of summertime minima has recently been hypothesized to result from  $\text{N}_2$  fixation because inputs of organic matter with low  $\delta^{15}\text{N}$  values from  $\text{N}_2$  fixation may overprint the effect of nutrient uptake on  $\delta^{15}\text{N}$  values [White *et al.*, 2007].

[8] The average  $\delta^{15}\text{N}$  values of bulk sediment in Guaymas Basin are thought to reflect denitrification primarily and are assumed to be influenced by the  $\delta^{15}\text{N}_{\text{nitrate}}$  values of upwelled water [Pride *et al.*, 1999]. Bulk sedimentary  $\delta^{15}\text{N}$  ( $\delta^{15}\text{N}_{\text{bulk}}$ ) values are high ( $>9\text{‰}$ ) due to the regional overprint of water column denitrification [Altabet *et al.*, 1999], but are not as high as the  $\delta^{15}\text{N}_{\text{nitrate}}$  values at specific depths. This difference results from  $\delta^{15}\text{N}_{\text{bulk}}$  values integrating the entire water column  $\delta^{15}\text{N}_{\text{PM}}$  and not just the maximum  $\delta^{15}\text{N}_{\text{nitrate}}$  values. Interannual variability in sediment trap  $\delta^{15}\text{N}_{\text{PM}}$  values and their temporal patterns suggest that processes other than denitrification may affect the  $\delta^{15}\text{N}_{\text{bulk}}$  values [Altabet *et al.*, 1999; White *et al.*, 2007].

### 1.3. Diatom-Bound $\delta^{15}\text{N}$ Values

[9] This paper explores the utility of using nitrogen isotope analyses of diatom-bound organic matter in

two distinct diatom size fractions to elucidate nitrogen cycling in the GoC. Diatom-bound  $\delta^{15}\text{N}$  measurements were originally developed as a way to measure sedimentary  $\delta^{15}\text{N}$  values that are not affected by alteration during sinking and burial [Robinson *et al.*, 2004; Shemesh *et al.*, 1993]. Diatoms produce a range of nitrogen bearing organic compounds, including polyamines, mycosporine-like amino acids, chitin, and proteins (silaffins and cingulins) that are permanently associated with the silica frustule [Brunner *et al.*, 2009; Ingalls *et al.*, 2010; Kroger *et al.*, 1999; Scheffel *et al.*, 2011]. As a result, diatom microfossils protect primary photosynthetic N formed in the surface ocean. However, alteration of the bulk sedimentary  $\delta^{15}\text{N}$  values is not a significant problem in the highly productive eastern tropical Pacific [Altabet *et al.*, 1999; Kienast *et al.*, 2002]. In this region, diatoms are targeted because they have the potential to be sensitive recorders of several N cycling processes in the GoC. For example, diatoms live in the surface waters where  $\text{N}_2$  fixation occurs and some species host  $\text{N}_2$ -fixing symbionts. As a result, surface dwelling diatoms may access regenerated nitrate from newly fixed  $\text{N}_2$  before it is completely mixed with the upwelled nitrate. In addition, the seasonality in diatom sizes may allow for separation of a “seasonal” signal: smaller diatoms characterize rapid growth periods associated with upwelling while the larger types are associated with “fall dump” and the stratified summer months [Altabet *et al.*, 1999; Kemp *et al.*, 2000; Sancetta, 1995; White *et al.*, 2007]. In this paper, we use the  $\delta^{15}\text{N}$  values of two size classes of diatoms to examine how groups of diatoms with different ecologies contribute to nitrogen cycling within the GoC. The results presented here indicate that additional source(s) of nitrate, beyond upwelling, help to drive high rates of export to the seafloor.

## 2. Methods

### 2.1. Sediment Cores and Sampling

[10] All sediment samples were from kasten core MD02–2517, recovered from the western Guaymas Basin (27°29.10 N, 112°04.46 W) (Figure 1) at a water depth of 881 m. The core depth corresponds to the base of the oxygen minimum zone [Beaufort *et al.*, 2002]. Six 8 cm long blocked intervals were used in this study: 133–141 cm, 208–216 cm, 247–255 cm, 330–338 cm, 447–455 cm, and 558–566 cm. Each block had the approximate dimensions of 11.5 cm by 8 cm by 5 cm in the x, y, and z

dimensions, respectively. Two of the sections, 133–141 cm and 208–216 cm, were homogenous, while the other four contained alternating lighter opal and darker silt laminae. Age estimates for each block are based on the age model from Cheshire *et al.* [2005] for the complementary piston core, MD02–2515, which has an error of  $\pm 1$  ky. The MD02–2515 age model was derived through correlation of laminae thickness and degree of bioturbation to the neighboring  $^{14}\text{C}$ -dated core JPC 56 [Cheshire *et al.*, 2005; Keigwin, 2002]. The six sediment sections were sampled in two manners. A vertical slice of every block was divided into 1 cm thick samples for comparison to traditional paleoceanographic sampling techniques. The four laminated sections were also sampled every 1 mm to 5 mm which resulted in a high-resolution record, on the order of half a year to 4 years based upon varve counting. It is assumed that each varve represents approximately half a year. Although the resolution is highest in mm-scale samples, the data will be discussed in terms of the general trends that are consistent between both sampling schemes (Figure S1 in the auxiliary material).<sup>1</sup> Multiple measurements, including weight percent opal (opal), weight percent organic carbon ( $\text{C}_{\text{org}}$ ),  $\delta^{15}\text{N}_{\text{bulk}}$ , and diatom-bound  $\delta^{15}\text{N}$  values of  $<63 \mu\text{m}$  and  $>63 \mu\text{m}$  size fractions, were made on each sample.

[11] Water column diatom samples were collected for comparison of modern diatom-bound  $\delta^{15}\text{N}$  values to the sediment-based measurements. The modern water column diatom samples were collected at seven stations within the GoC and eastern tropical Pacific from the RV New Horizon during July of 2008. Approximately 150 L of water were collected by closing multiple sample bottles on the CTD rosette at the sample depth. The water was then filtered through a 5.0  $\mu\text{m}$  polycarbonate filter. The water was collected from the surface at two of the stations and from the DCM at the remaining five stations. The filters were frozen for later analysis. Each station produced one sample used for diatom-bound  $\delta^{15}\text{N}$  analysis. The  $\delta^{15}\text{N}_{\text{PM}}$  values were determined on 2 L samples collected through the upper water column at each station.

### 2.2. Analytical Procedures

[12] Opal was measured colorimetrically using UV/Vis spectrophotometry (Simadzu, UV mini 1240) [DeMaster, 1981; Mortlock and Froelich, 1989]. Replicate samples of each dissolution step indicate

<sup>1</sup>Auxiliary materials are available in the HTML. doi:10.1029/2010GC003437.

that the standard deviation was 1.5%. Organic carbon and total nitrogen concentrations and bulk N isotope values were measured by flash combustion using a Costech 4010 elemental analyzer coupled to an isotope ratio mass spectrometer (Thermo, Delta V) (EA-IRMS). For  $C_{\text{org}}$  measurements, samples were acidified with sulfurous acid prior to combustion [Verardo *et al.*, 1990]. The concentration measurements were calibrated using an in-house amino-caproic acid (ACA) standard. The bulk sediment isotope measurements were calibrated using the ACA standard and internationally recognized reference materials, measured in parallel with samples. The reference materials were IAEA-N1 and N2 ammonium sulfate ( $\delta^{15}\text{N} = 0.4$  and  $20.3\text{‰}$ , versus AIR, respectively). Standard deviation based on multiple analyses of the reference materials was  $\pm 0.3\text{‰}$  for  $\delta^{15}\text{N}_{\text{bulk}}$ . The range between replicates for  $C_{\text{org}}$  was  $\pm 0.3\%$  or better and for total nitrogen the range was  $\pm 0.02\%$  or better.

[13] Diatom-bound organic matter was prepared for nitrogen isotopic analyses using methods adapted from Robinson *et al.* [2004] and Robinson and Sigman [2008] (see Text S1, Figure S2, and Figure S3). To remove excess organic matter before physical separation, approximately 0.3 g of dry sample was oxidized at room temperature using saturated potassium permanganate, 50% sulfuric acid and saturated oxalic acid [Hasle and Fryxell, 1970] (Figure S2). The oxidized sample was sieved at  $63\ \mu\text{m}$  and the two size fractions ( $<63\ \mu\text{m}$  and  $>63\ \mu\text{m}$ ) were cleaned separately as described by Robinson *et al.* [2004] and Robinson and Sigman [2008] (see Text S1, Figure S2, and Figure S3) with slight modifications. The  $>63\ \mu\text{m}$  fraction was not settled in sodium lauryl sulfate solution due to the small sample size and negligible clay. The reductive cleaning step was followed by a repeat of the potassium permanganate oxidation [Hasle and Fryxell, 1970] rather than using heated hydrogen peroxide for a secondary oxidation. The final oxidation used concentrated perchloric acid, at  $100^\circ\text{C}$ . This step was repeated four times for the  $<63\ \mu\text{m}$  fraction (Figure S3). For the  $>63\ \mu\text{m}$  fraction only a single perchloric oxidation was needed.

[14] N content and  $\delta^{15}\text{N}$  values were measured on the clean, dry diatom samples using the methods of Robinson *et al.* [2004] and Robinson and Sigman [2008]. Diatom bound organic nitrogen is released and converted to nitrate by an alkaline persulfate oxidation. Nitrate concentrations were determined by chemiluminescence [Braman and Hendrix, 1989] on a Teledyne model 200E NOx.

The  $\delta^{15}\text{N}_{\text{nitrate}}$  values were determined using the denitrifier method on a Thermo Scientific Delta V isotope ratio mass spectrometer [Sigman *et al.*, 2001]. All  $\delta^{15}\text{N}_{\text{nitrate}}$  values are reported relative to air and were normalized to IAEA-NO-3 ( $4.7\text{‰}$ ) [Gonfiantini *et al.*, 1995]. Based upon replicates analyzed with each set of cleanings, the standard deviation for the  $<63\ \mu\text{m}$  size fraction was  $\pm 1\text{‰}$  and the  $>63\ \mu\text{m}$  size fraction was  $\pm 1.7\text{‰}$ .

[15] The water column samples were prepared and analyzed using the same procedure as the sediments with a few exceptions. Filters were soaked in sodium lauryl sulfate overnight to remove as much sample as possible from the filter. Due to the small size, the entire sample was analyzed at one time, precluding replicate measurements. The samples were then taken through the diatom-bound chemical cleaning as described above which included the reduction, permanganate oxidation, and perchloric oxidation. Similar to the  $>63\ \mu\text{m}$  size fraction, the water column samples were only treated once with perchloric acid at  $100^\circ\text{C}$ . The water column diatom bound  $\delta^{15}\text{N}$  values were measured according to the procedure described above. The error is estimated to be approximately the same as for the  $>63\ \mu\text{m}$  samples, given similar sample sizes and cleaning methods.

### 2.3. Diatom Identification

[16] Diatoms from the  $>63\ \mu\text{m}$  size fraction were identified and qualitatively counted to determine if “fall dump” species were present and if so, their relative abundance. Using a light microscope at  $400\times$  magnification, large *Coscinodiscus* species (*C. asteromphalus* and *C. oculus-iridis*) associated with the fall dump [Kemp *et al.*, 2000] were identified. *Thalassiothrix longissima* was identified primarily by length: if the diatom was longer than  $250\ \mu\text{m}$  and less than  $6\ \mu\text{m}$  wide it was considered to be *T. longissima* and was counted. However, diatom counts are likely qualitative because fragments may have been counted more than once. The two large *Coscinodiscus* species (*C. asteromphalus* and *C. oculus-iridis*) were identified based upon size and the unique arrangement of the center areole.

## 3. Results

[17] All sediment samples were opal- (20–50%) and organic carbon-rich (2–4.5%) (Figures 2 and 3). The diatom-bound  $\delta^{15}\text{N}$  values of the  $>63\ \mu\text{m}$  size fraction ( $\delta^{15}\text{N}_{\text{large}}$ ) were substantially lower than the  $<63\ \mu\text{m}$  size fraction ( $\delta^{15}\text{N}_{\text{small}}$ ) in all

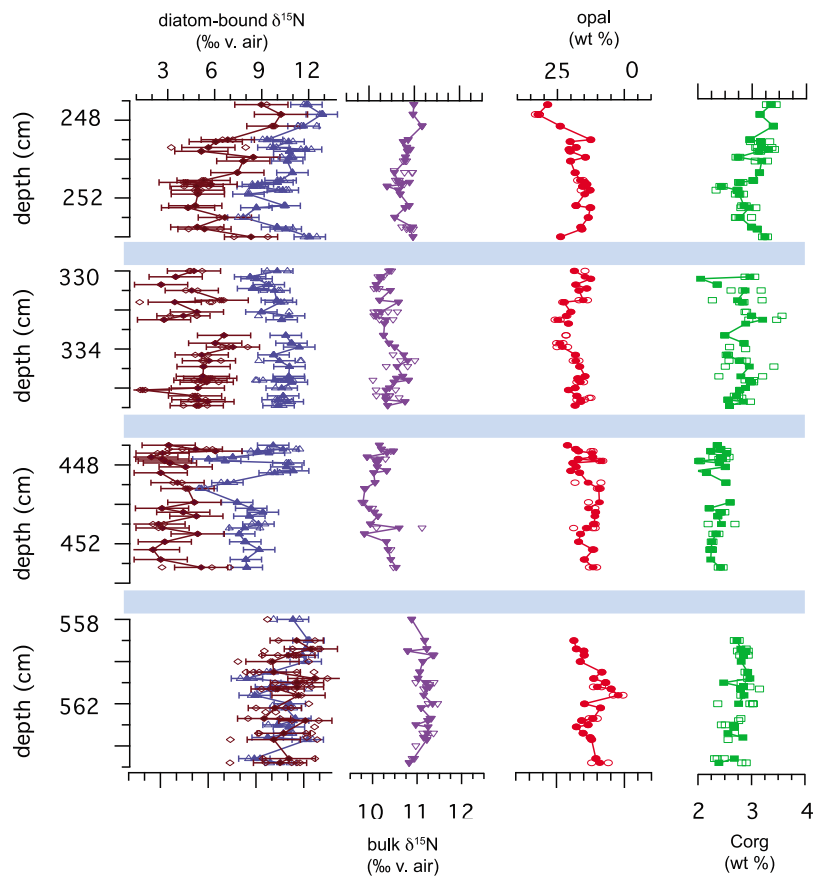


**Figure 2.** Down section profiles of  $\delta^{15}\text{N}_{\text{large}}$  (diatom bound from  $>63 \mu\text{m}$  size fraction; maroon diamonds),  $\delta^{15}\text{N}_{\text{small}}$  (diatom bound from  $<63 \mu\text{m}$  size fraction; blue triangles),  $\delta^{15}\text{N}_{\text{bulk}}$  (purple triangles), weight percent opal (red circles), and weight percent organic carbon (green squares) sampled at mm scale from the four laminated sections. The closed markers are the averages, and the open markers represent the replicates. Note that these are sections with large, unsampled gaps between them, not a continuous core.

sections except the oldest, 558–566 cm (Figures 2 and 3). The  $\delta^{15}\text{N}_{\text{small}}$  values ranged from 7 to 12‰ and  $\delta^{15}\text{N}_{\text{large}}$  ranged from 1 to 7‰ except in the oldest section. The  $\delta^{15}\text{N}_{\text{bulk}}$  values had a much smaller range of 10–11.5‰ (Figures 2 and 3). This could be due, at least in part, to the larger error associated with the diatom-bound analyses. The  $<63 \mu\text{m}$  fraction was made up primarily of winter species such as *Fragilariopsis doliolus* and other small pennate diatoms. Based upon individuals counted, *T. longissima*, a mat forming and “fall dump” species, was estimated to make up between 30 and 95% of the  $>63 \mu\text{m}$  diatoms in the laminated sections (Figure S4). In the two homogenous sections, the large centric diatoms, *C. asteromphalus*, and *C. oculus-iridis*, associated with the “fall dump” assemblage [Kemp et al., 2000], accounted for 10–25%.

[18] The water column diatom-bound  $\delta^{15}\text{N}$  values were significantly lower than the  $\delta^{15}\text{N}_{\text{PM}}$  values

(7–11‰) measured throughout the water column (Figures 4 and S5). The two water column diatom-bound  $\delta^{15}\text{N}$  values collected from  $<10 \text{ m}$  water depth had  $\delta^{15}\text{N}$  values of 7.7 and 3.1‰, whereas the samples collected deeper than 10 m ranged from 1.7 to  $-9.7$ ‰ (Figures 4 and S5). Microscopic analysis at 3 stations revealed differences in the opaline plankton. Station 11 had abundant silica-flagellates, station 9 was dominated by a small, unidentified centric diatom species, and station 12 was dominated by a long thin diatom, likely *T. longissima* (Figures 1, 4, and S4). Station 12 also had the highest fucoxanthin:chlorophyll ratio, which ranged from 0.5 to 0.8 throughout the upper 50 m (A. White, personal communication, 2008, data not shown) indicating that diatoms were more dominant at this station than the others. At station 12 the  $\delta^{15}\text{N}_{\text{PM}}$  values average  $\sim 11$ ‰ at the surface and decreased to  $\sim 8.5$ ‰ in the DCM (Figure 4). Concurrently, the diatom-bound  $\delta^{15}\text{N}$  value taken

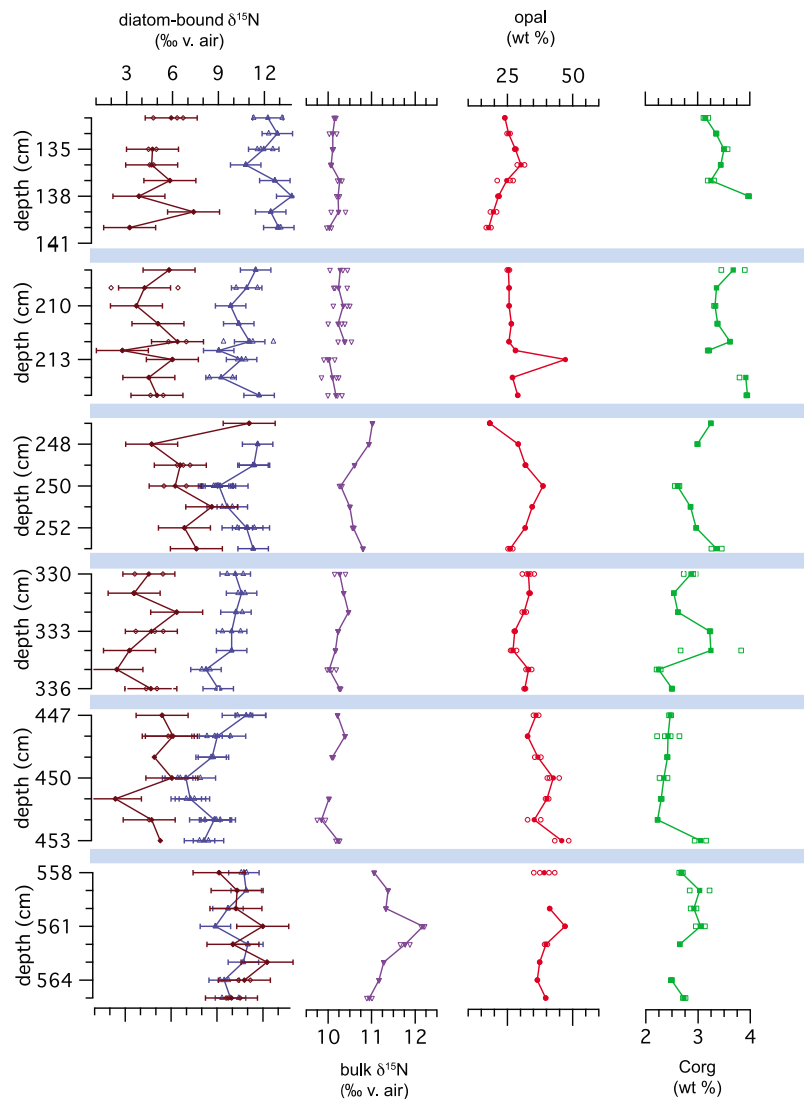


**Figure 3.** The  $\delta^{15}\text{N}_{\text{large}}$  (maroon diamonds),  $\delta^{15}\text{N}_{\text{small}}$  (blue triangles),  $\delta^{15}\text{N}_{\text{bulk}}$  (purple triangles), opal (red circles), and  $\text{C}_{\text{org}}$  (green squares) from all six sections sampled every cm. The closed markers are the average values, and the open markers represent the replicates. Again, note that these are sections and not a continuous core. The centimeter sampling shows lower frequency and lower amplitude changes than the finer millimeter scale scheme (Figure S1).

from the upper portion of the DCM had a value of  $-0.4 \pm 1.7\text{‰}$ .

[19] The sediment data were analyzed using a Spearman correlation analysis. The centimeter scale and millimeter-scale data were evaluated separately to avoid breaking assumptions of the test. Correlation existed between opal,  $\text{C}_{\text{org}}$  and  $\delta^{15}\text{N}_{\text{small}}$  values in both the mm and cm samples. Opal content was negatively correlated to both  $\text{C}_{\text{org}}$  content and  $\delta^{15}\text{N}_{\text{small}}$  values ( $r_{\text{cm}}$ :  $-0.79$ ;  $-0.57$  and  $r_{\text{mm}}$ :  $-0.44$ ;  $-0.47$  respectively) whereas  $\text{C}_{\text{org}}$  and  $\delta^{15}\text{N}_{\text{small}}$  values were positively correlated ( $r_{\text{cm}}$ :  $0.70$  and  $r_{\text{mm}}$ :  $0.49$ ) (Table 1). These relationships were visually apparent in each plot, as were low

frequency variations throughout the sections (Figures 2 and 3). Although not obvious, there was also a strong correlation between  $\delta^{15}\text{N}_{\text{bulk}}$  and  $\delta^{15}\text{N}_{\text{large}}$  values ( $r_{\text{cm}}$ :  $0.68$  and  $r_{\text{mm}}$ :  $0.82$ ).

## 4. Discussion

### 4.1. Separating the Controls on Sedimentary $\delta^{15}\text{N}$ Values

[20] Throughout the discussion we use sediment opal concentration as a proxy for diatom productivity. Sediment trap data show opal content and flux to be strongly positively correlated to CZCS

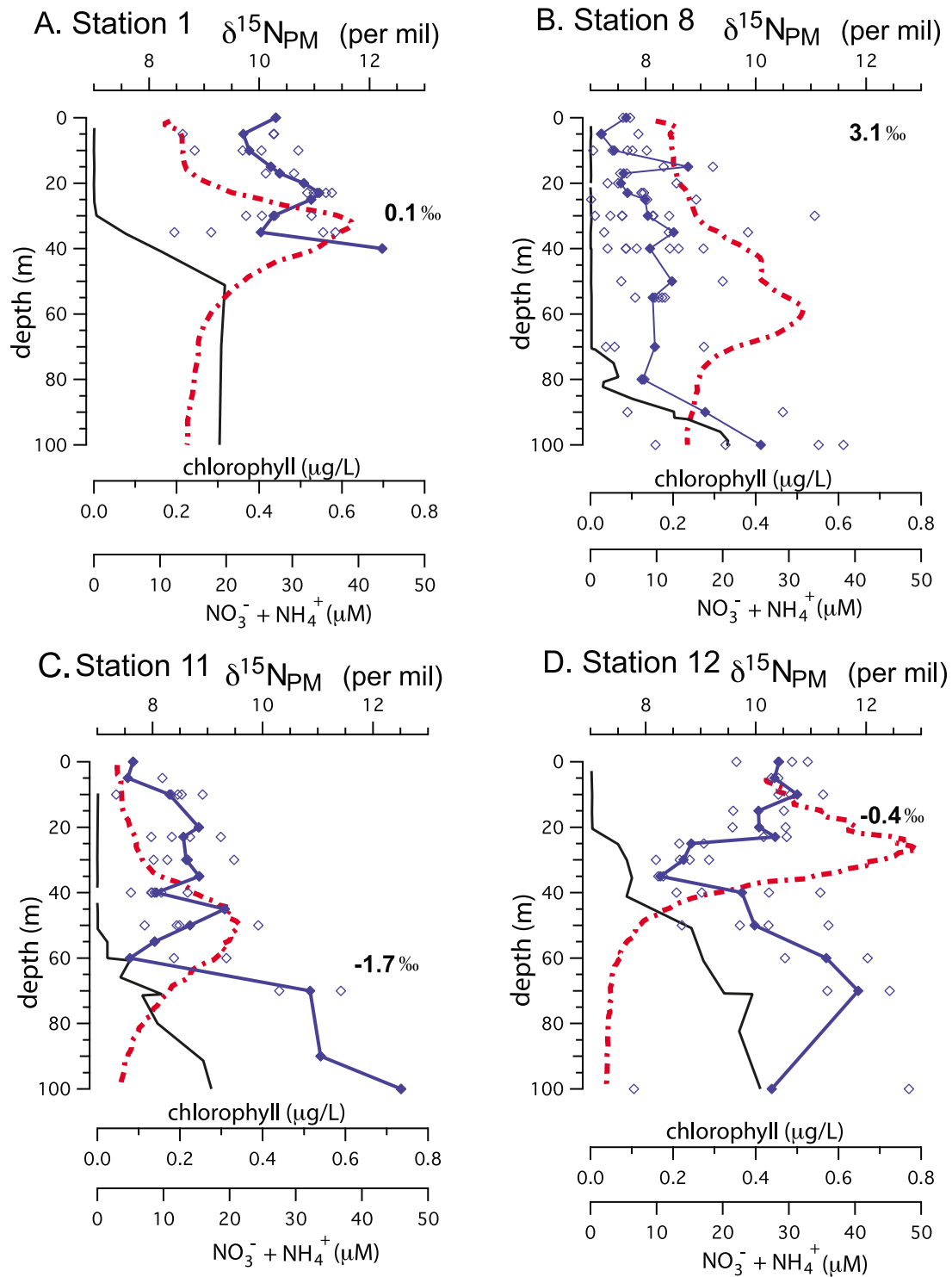


**Figure 4.** Chlorophyll (red dashed line), nitrate and ammonium (black solid line),  $\delta^{15}\text{N}$  values of particulate matter (blue closed diamonds are average values, and open diamonds are measured values), and the water column diatom-bound  $\delta^{15}\text{N}$  values are in black bold font on the right of the graph. All  $\delta^{15}\text{N}$  values are reported in per mil (‰) versus air. The diatom-bound  $\delta^{15}\text{N}$  value is placed at the sample depth with an estimated error of  $\pm 1.7\text{‰}$  (not shown). The geographic locations of the stations are shown in Figure 1. These four stations are representative of all the locations, and the data from the additional three stations are shown in Figure S5.



**Table 1.** Spearman Correlation Coefficient Matrices<sup>a</sup>

Opal	$\delta^{15}\text{N}_{\text{bulk}}$	$C_{\text{org}}$	$\delta^{15}\text{N}_{\text{small}}$	$\delta^{15}\text{N}_{\text{large}}$
<i>Correlation Coefficients From Centimeter Samples</i>				
1	NS	-0.79 <sup>b</sup>	-0.57 <sup>b</sup>	NS
NS	1	NS	NS	0.68 <sup>b</sup>
-0.79 <sup>b</sup>	NS	1	0.70 <sup>b</sup>	NS
-0.57 <sup>b</sup>	NS	0.70 <sup>b</sup>	1	NS
NS	0.68 <sup>b</sup>	NS	NS	1
<i>Correlation Coefficients From Millimeter Sample</i>				
1	NS	-0.44 <sup>b</sup>	-0.49 <sup>b</sup>	NS
NS	1	0.49 <sup>b</sup>	0.53 <sup>b</sup>	0.82 <sup>b</sup>
-0.44 <sup>b</sup>	0.49 <sup>b</sup>	1	0.47 <sup>b</sup>	0.41
-0.49 <sup>b</sup>	0.53 <sup>b</sup>	0.47 <sup>b</sup>	1	0.53 <sup>b</sup>
NS	0.82 <sup>b</sup>	0.41 <sup>b</sup>	0.53 <sup>b</sup>	1

<sup>a</sup>NS, not significant.

<sup>b</sup>Significance of <0.0001; coefficients without a footnote are significant to <0.01.

satellite-derived chlorophyll concentration during the annual cycle with significant peaks during winter when upwelling occurs. Both in this study and in *Thunell's* [1998] sediment trap work, the concentration of  $C_{\text{org}}$  varies inversely with opal content. The  $C_{\text{org}}:\text{N}_{\text{total}}$  molar ratio (9–13) suggest that the sedimentary organic matter is of marine origin implying the inverse relationship between the concentrations of  $C_{\text{org}}$  and opal is due to dilution by opal.

#### 4.1.1. The $\delta^{15}\text{N}_{\text{bulk}}$ Values

[21] The low variability of  $\delta^{15}\text{N}_{\text{bulk}}$  values suggests a relatively stable N cycle during the sample interval (Figures 2 and 3). Profiles of sedimentary  $\delta^{15}\text{N}_{\text{bulk}}$  values from the Guaymas Basin have been generally interpreted as variations in the  $\delta^{15}\text{N}_{\text{nitrate}}$  in the subeuphotic zone which is controlled by the extent of denitrification. Another possibility is that  $\delta^{15}\text{N}_{\text{bulk}}$  values record inputs of low  $\delta^{15}\text{N}$ , N resulting from  $\text{N}_2$  fixation or changes in nitrate availability, that overprint the subsurface denitrification signal. The small range of  $\delta^{15}\text{N}_{\text{bulk}}$  values (~2‰) observed here indicates that there were not large changes in the N cycle during the sample interval. This is in contrast to longer intervals that span climate events, including the transition from the last glacial maximum to the Holocene when  $\delta^{15}\text{N}_{\text{bulk}}$  values varied by 3–7‰ [Pride *et al.*, 1999].

#### 4.1.2. The $\delta^{15}\text{N}_{\text{small}}$ Values

[22] When analyzed in combination with opal content and diatom assemblages, the  $\delta^{15}\text{N}_{\text{small}}$  values appear to be recording a nutrient utilization signal. The <63  $\mu\text{m}$  fraction is composed of diatom species associated primarily with the winter-spring

upwelling bloom. Like  $\delta^{15}\text{N}_{\text{bulk}}$  values, changes in the values of  $\delta^{15}\text{N}_{\text{small}}$  could be associated with variation in subeuphotic zone  $\delta^{15}\text{N}_{\text{nitrate}}$  values. In Guaymas Basin over the course of a year, nitrate in the upper surface mixed layer is typically completely consumed [Altabet *et al.*, 1999; White *et al.*, 2007]. Therefore no fractionation between source N (nitrate) and product (diatom-bound organic matter) is expected in an annually integrated sample. However, this may not be true if the smaller diatoms are biased toward the upwelling season. The occurrence of low values of  $\delta^{15}\text{N}_{\text{small}}$  may reflect enhanced supply of nutrients relative to demand. If  $\delta^{15}\text{N}_{\text{small}}$  values reflect changes in the extent of nitrate consumption, then opal concentrations would likely be negatively correlated with  $\delta^{15}\text{N}_{\text{small}}$ . Higher nitrate concentrations are associated with periods of higher diatom productivity and higher sedimentary opal concentrations in sediment trap studies [Altabet *et al.*, 1999; Pride *et al.*, 1999]. We extend this interpretation to  $\delta^{15}\text{N}_{\text{small}}$ , and assert that variability in the supply and demand of nitrate explains the negative correlation between  $\delta^{15}\text{N}_{\text{small}}$  and opal contents. In addition, the sediment trap data from Guaymas Basin show a similar relationship, with peaks in opal concentrations corresponding to low values of  $\delta^{15}\text{N}_{\text{PM}}$  [Pride *et al.*, 1999].

[23]  $\text{N}_2$  fixation could also explain the negative correlation between  $\delta^{15}\text{N}_{\text{small}}$  and opal, however, the absence of diatoms associated with  $\text{N}_2$  fixation and the location of the core do not support this interpretation.  $\text{N}_2$  fixation by diazotrophic symbionts within diatoms, such as *Richelia* with *Rhizoselenia spp.* or *Hemialus spp.*, could increase opal production and decrease values of  $\delta^{15}\text{N}_{\text{small}}$ . *Rhizoselenia* was not observed in the sediment, likely because it is lightly silicified and rarely preserved. *Rhizoselenia's* poor preservation makes it unlikely that  $\text{N}_2$  fixation-stimulated diatom blooms contribute to high opal concentrations in the sediment. Additionally,  $\text{N}_2$  fixation has only been documented during summer when surface mixed layer nitrate concentrations were extremely low [White *et al.*, 2007]. Thus we do not expect  $\text{N}_2$  fixation to be associated with the upwelling/bloom related diatoms in the <63  $\mu\text{m}$  fraction or to increase with opal content. Moreover, kasten core MD02–2517 was recovered from the western Guaymas Basin, where White *et al.* [2007] did not measure significant rates of  $\text{N}_2$  fixation. They argued, based on an analysis of a 5 year time series of satellite nighttime sea surface temperatures and chlorophyll concentrations, that  $\text{N}_2$  fixation blooms are not a common feature of the western

margin of the GoC. While it is incorrect to dismiss  $N_2$  fixation as a possible explanation of the  $\delta^{15}N_{\text{small}}$  values, the data available indicate that  $\delta^{15}N_{\text{small}}$  values largely reflect nutrient availability along the western coast of the GoC. We should note that  $\delta^{15}N_{\text{small}}$  values from the central or eastern GoC, where  $N_2$  fixation appears to be a more common summertime phenomenon [White *et al.*, 2007], could record a  $N_2$  fixation signal.

#### 4.1.3. The $\delta^{15}N_{\text{large}}$ Values

[24] Significantly lower values of  $\delta^{15}N_{\text{large}}$  (by  $\sim 4\text{--}6\%$ ) in all sections, except the oldest (558–566 cm), suggest that larger diatoms record a distinct source of N isotope variability within the GoC (Figures 2 and 3). Several processes are potentially responsible, including (1) different isotopic fractionations between species, (2) the incorporation of newly fixed nitrogen, (3) N cycling that is not representative of the GoC, and/or (4) excess nutrient availability from living in the subsurface combined with lower isotope fractionation due to low light conditions [DiFiore *et al.*, 2006; Needoba and Harrison, 2004].

[25] The fractionation associated with the incorporation of N into organic compounds within the diatom frustules is not well studied. It is not known how variable the N fractionation is between diatom species or within the same species. The only existing N isotope data are from laboratory culture experiments that focus on polar diatom species. The data indicate that there is a fractionation and the N within the frustules is typically  $5.3 \pm 4.4\%$  less than the bulk biomass [Horn *et al.*, 2011]. A weak correlation ( $r = 0.43$ ,  $n = 6$ ) between size and the magnitude of this fractionation is observed, where larger diatoms tended to have a smaller offset between the bulk biomass and the N contained within the frustule. The  $>63\ \mu\text{m}$  size fraction of some sediment samples was dominated by what appears to be a single species, *T. longissima*, and it is possible that *T. longissima* has a higher isotopic fractionation associated with frustule construction causing the  $\delta^{15}N_{\text{large}}$  values to be low. This is opposite to the size related trend observed in culture. In addition, sections with more variable assemblages also bear significantly lower  $\delta^{15}N_{\text{large}}$  values than the bulk sediment. Finally, *T. longissima* dominated the interval that lacked an offset between the  $\delta^{15}N_{\text{large}}$  and  $\delta^{15}N_{\text{small}}$  values. Assemblage alone cannot control the  $\delta^{15}N_{\text{large}}$  values.

[26] Another possibility is that the “fall dump” species, which were abundant in  $\delta^{15}N_{\text{large}}$  samples,

were heavily biased by  $N_2$  fixation inputs associated with summer stratification. However, water column data do not support this as the primary reason for the low  $\delta^{15}N_{\text{large}}$  values. In the summer of 2008, only minimal rates of  $N_2$  fixation were measured and the  $\delta^{15}N_{\text{PM}}$  values were generally higher (7–12‰) than the  $\delta^{15}N_{\text{PM}}$  values (5–6‰) in 2005 when in situ rates of  $N_2$  fixation were high [White *et al.*, 2007] (Figure 4). Despite the lack of evidence for  $N_2$  fixation during the summer of 2008, the water column diatom-bound  $\delta^{15}N$  values were low. This may be in part due to differences between fresh diatom-bound and sedimentary diatom-bound  $\delta^{15}N$  values (see section 4.1.4). However, the water column diatom-bound  $\delta^{15}N$  values from samples recovered at depth (15–50 m) are consistently lower than surface (0–5 m) diatom-bound samples, suggesting that this is not the only cause. The lack of measurable fixation and the decrease in modern diatom-bound  $\delta^{15}N$  values with depth, together with the location of the core, along the western coast where  $N_2$  fixation is not expected to be common [White *et al.*, 2007], suggest the low  $\delta^{15}N_{\text{large}}$  values cannot be easily attributed to  $N_2$  fixation. Although, we predicted that  $N_2$  fixation could be recorded by fall dump species and  $N_2$  fixation might explain some of the sediment observations, it does not provide a complete explanation for our observations.

[27] A third possibility is the  $\delta^{15}N_{\text{large}}$  values are recording a signal unrelated to the large scale N cycling within the GoC. The low  $\delta^{15}N_{\text{large}}$  values are associated with the mat forming species, *T. longissima*. It is possible that the N within the microenvironment of the mat is drawn down to such an extent that  $N_2$  fixation occurs within the mat that would not otherwise occur. But, again, the low  $\delta^{15}N_{\text{large}}$  values are not exclusive to *T. longissima* dominated samples. Alternatively, if *T. longissima* is transported into the GoC the  $\delta^{15}N_{\text{large}}$  values may be recording nitrogen cycling processes from outside to the GoC. Pike and Kemp [1997] interpreted the *T. longissima* mats to be of allochthonous origin in their investigation of the laminations in Guaymas Basin. *T. longissima* has been classified as an arctic to temperate species from the Northern Hemisphere [Hasle, 2001] and the mats were postulated to have entered the GoC with Pacific water during summer at the surface or along pycnoclines [Pike and Kemp, 1997]. The lower  $\delta^{15}N_{\text{large}}$  values may represent utilization of a substrate pool from a zone where the extent of denitrification was much lower than that in the GoC. If *T. longissima* were transported into the GoC then the sediments incorporated significant

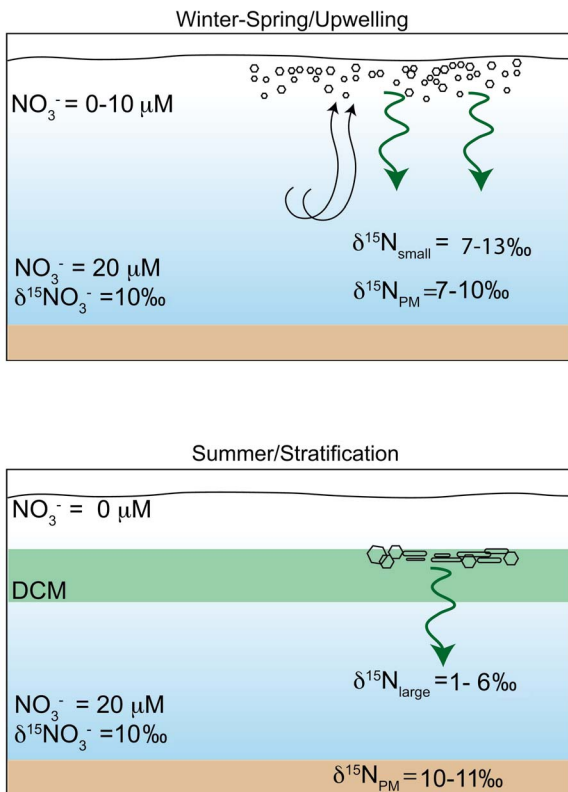


**Figure 5.** Summary diagram of sedimentary results and interpretations. (top) The incorporation of  $^{15}\text{N}$  into small diatoms during the winter-spring upwelling season. (bottom) Summertime, stratified conditions with diatoms living at the DCM. These are likely “fall dump” diatoms living at the nitracline, under nutrient-replete, low light conditions that result in the export of organic matter with low  $\delta^{15}\text{N}$  values to the seafloor. The  $\delta^{15}\text{N}_{\text{PM}}$  values are representative of sediment trap data from *Altabet et al.* [1999].

amounts of opal and  $\delta^{15}\text{N}$  values from outside of the GoC [*Pike and Kemp, 1997*]. On the other hand, *T. longissima* occurs consistently throughout the sampled sections, not sporadically, strongly suggesting that they grow locally and were not imported from outside of the GoC.

[28] The most complete explanation for the low  $\delta^{15}\text{N}_{\text{large}}$  values is that the diatoms grew where nitrate was abundant and light levels were low. The water column diatom-bound  $\delta^{15}\text{N}$  data support this hypothesis. The lowest water column diatom-bound  $\delta^{15}\text{N}$  values were recorded by samples taken within the DCM, at or just above the nitracline. The high nitrate availability would allow diatoms to preferentially incorporate  $^{14}\text{NO}_3^-$ , leading to an enhanced expression of the isotopic fractionation and lower  $\delta^{15}\text{N}$  values. The DCM sits between 30 and 70 m water depth, which corresponds to lower

light levels. During 2004–2005 seasonal cruises in the GoC, the light levels at 30 m were commonly less than  $50\text{--}75 \mu\text{Ein m}^{-2} \text{s}^{-1}$  (B. Popp, unpublished data, 2005). For diatoms grown in culture, low light conditions ( $10\text{--}15 \mu\text{Ein m}^{-2} \text{s}^{-1}$ ) have been shown to increase isotope fractionation associated with the uptake and assimilation of nitrate ( $\epsilon_{\text{nitrate}}$ ) up to threefold when compared to high light conditions ( $140 \mu\text{Ein m}^{-2} \text{s}^{-1}$ ) [*Needoba and Harrison, 2004*]. Additional, in situ evidence for this effect comes from a water column study of the isotopic composition of nitrate across the Southern Ocean [*DiFiore et al., 2006*]. A higher  $\epsilon_{\text{nitrate}}$  would lead to lower  $\delta^{15}\text{N}$  values in the product, which in this case is the diatom. Both the excess  $\text{NO}_3^-$  and low light conditions would work together to lower the  $\delta^{15}\text{N}$  values in diatoms living at depth (Figure 5).

[29] One of the most striking differences between sections is the high  $\delta^{15}\text{N}_{\text{large}}$  values in section 558–566 cm (Figures 2 and 3). The age model, based on a stratigraphic correlation between core JPC-56 and a complimentary piston core MD02–2515, places the oldest block at approximately 10 ky. It should be stressed that this is not a precise date. Nonetheless, 10 ky ago was a period of large scale circulation changes prior to the onset of the stable Holocene [*Pride et al., 1999*]. In core JPC-56, at 10 ky there is a sharp increase in opal which remains high until  $\sim 6$  ky [*Pride et al., 1999*]. Additionally, *Cyclotella spp.*, diatoms associated with warm-stratified nutrient-poor waters, were dramatically reduced until  $\sim 10$  ky, indicating that the summer surface waters were not as stratified [*Barron et al., 2005*]. The similarity between the  $\delta^{15}\text{N}_{\text{small}}$  and the  $\delta^{15}\text{N}_{\text{large}}$  may simply reflect this enhanced mixing and overall reduction in upper water column structure. Without better age control and additional sample analysis, it is difficult to determine the cause of the uniform  $\delta^{15}\text{N}$  values across size fractions in this sediment section.

[30] The observed correlation between values of  $\delta^{15}\text{N}_{\text{bulk}}$  and  $\delta^{15}\text{N}_{\text{large}}$  implies that the biomass produced by the large diatoms that presumably grew at depth influences the  $\delta^{15}\text{N}_{\text{bulk}}$  values. There are two important implications of this correlation. First, the contributions to bulk N from the deep dwelling diatoms may cause small changes in the  $\delta^{15}\text{N}_{\text{bulk}}$ . Second, the correlation indicates that deep dwelling diatoms using nitrogen from the nitracline may represent a significant source of export production that is not associated with the winter upwelling season. The correlation between values of  $\delta^{15}\text{N}_{\text{large}}$  and  $\delta^{15}\text{N}_{\text{bulk}}$  provides support of pre-

vious work, which suggests large diatoms, such as *T. longissima*, increase export production [Kemp et al., 2000; Pike and Kemp, 1997; Sancetta et al., 1991; Shimada et al., 2008]. A first order approximation of the total nitrogen exported to the sediment by the large diatoms is 3–15% of total N in the bulk sediment. This approximation is based on the relative contributions of large diatoms to the total silica load, and assuming a Si-to-N ratio (Si:N) of 1.2 [Brzezinski, 1985], and normalized to total sedimentary nitrogen for each sample (Text S2). A Si:N ratio of 1.2 is the average of species that are greater than 20  $\mu\text{m}$ , derived from culture experiments. These same culture experiments showed that the Si:N value can vary between 0.41 and 2.17 and is species dependent [Brzezinski, 1985]. In a similar fashion, using the opal and the mass of large diatoms per gram of sediment, we estimate large diatoms contribute between 7 and 30% of the sedimentary opal. Further water column and sediment trap work is necessary to be able to quantify more precisely the extent to which these deep-dwelling diatoms influence export.

#### 4.1.4. Diatom-Bound $\delta^{15}\text{N}$ Values From the Water Column

[31] To our knowledge, these are the first diatom-bound  $\delta^{15}\text{N}$  values reported from water column samples, and they are much lower than diatom-bound  $\delta^{15}\text{N}$  values seen in sediment. The low water column diatom-bound  $\delta^{15}\text{N}$  values agree with culture experiments, which showed bulk biomass to be consistently higher than diatom-bound  $\delta^{15}\text{N}$  values [Horn et al., 2011]. The reverse, where diatom-bound is greater than bulk sediment  $\delta^{15}\text{N}$  values is commonly observed in sediment samples from the high latitude oceans [Robinson et al., 2004, 2005]. This difference suggests that a fraction with low  $\delta^{15}\text{N}$  values retained in diatom-bound samples grown in culture is lost during early diagenesis [Horn et al., 2011]. Similar to culture, the water column diatom-bound  $\delta^{15}\text{N}$  values, which are low relative to the  $\delta^{15}\text{N}$  values of nitrate and bulk sediments, likely have not experienced the loss of a  $^{15}\text{N}$ -depleted component of diatom bound organic matter. It is important to note here, that the dominant signal in the downcore diatom-bound nitrogen isotope records still appears to be changes in the  $\delta^{15}\text{N}_{\text{nitrate}}$  (M. Horn et al., manuscript in preparation, 2011). In the well preserved sediments of Guaymas Basin, diatom-bound  $\delta^{15}\text{N}_{\text{small}}$  values tend to be 1‰ less than  $\delta^{15}\text{N}_{\text{bulk}}$  in the opal-rich laminated intervals. In contrast values of  $\delta^{15}\text{N}_{\text{small}}$  are greater than  $\delta^{15}\text{N}_{\text{bulk}}$  values in the homoge-

neous intervals with lower opal contents, particularly for the sediment interval from 133 to 141 cm (Figure S6). This change in the diatom bound offset might be in part due to varying degrees of preservation of the initial diatom-bound  $\delta^{15}\text{N}$  values. More water column diatom-bound nitrogen isotope analyses are required to determine if low water column diatom-bound  $\delta^{15}\text{N}$  values are a universal feature or unique to the GoC. Additionally a more robust assessment of the effect of variable preservation on diatom-bound  $\delta^{15}\text{N}$  values and the resulting paleo reconstructions is needed.

## 4.2. Conclusions

[32] Multiple sediment size fraction and water column measurements of diatom-bound  $\delta^{15}\text{N}$  values indicate that large “fall dump” diatoms are important monitors of the nitrogen cycle and contribute to export production within the GoC. In all but one interval, the diatom-bound  $\delta^{15}\text{N}_{\text{large}}$  values, associated with fall dump species, were significantly lower than the diatom-bound  $\delta^{15}\text{N}_{\text{small}}$  values. Comparing sediment data to water column diatom-bound  $\delta^{15}\text{N}$  and  $\delta^{15}\text{N}_{\text{PM}}$  values suggests that the offset between  $\delta^{15}\text{N}_{\text{small}}$  and  $\delta^{15}\text{N}_{\text{large}}$  values is at least partially caused by diatoms growing at the nitracline under low light levels. Moreover, lower modern  $\delta^{15}\text{N}_{\text{PM}}$  values within the DCM and the correlation between values of  $\delta^{15}\text{N}_{\text{large}}$  and  $\delta^{15}\text{N}_{\text{bulk}}$  in the sediment indicate that production at depth can subtly contribute to the  $\delta^{15}\text{N}_{\text{bulk}}$  values. Furthermore, the correlation between values of  $\delta^{15}\text{N}_{\text{large}}$  and  $\delta^{15}\text{N}_{\text{bulk}}$  in the sediment stresses the importance of large diatoms to export production. We estimate that deep dwelling diatoms contribute 3–15% of the nitrogen in the sediment. These conclusions highlight the need to better understand bloom dynamics and the transport of large diatom species both inside and outside the GoC. Although the sedimentary diatom-bound  $\delta^{15}\text{N}$  data did not provide strong evidence for  $\text{N}_2$  fixation, this may be a result of location and the physical processes controlling stratification. Applying the diatom-bound  $\delta^{15}\text{N}$  measurements to various size fractions on a continuous core, along with other productivity proxies, will likely highlight changes in the N cycle on glacial-interglacial and decadal time scales that cannot be distinguished with  $\delta^{15}\text{N}_{\text{bulk}}$  measurements alone.

## Acknowledgments

[33] Initial conception of this work came from conversations between R.S.R. and E. Galbraith. E.G. also provided the sediment blocks. Special thanks to M. Horn and J. Brockmann

for their assistance in the laboratory. A. E. White and F. G. Prahl provided water column chlorophyll, pigment, and nutrient concentrations. They also provided constructive comments on an earlier version of this manuscript. J. A. Barron provided assistance with diatom identifications. The work was funded by ACS-PRF grant 46695-G2 to RSR and the Graduate School of Oceanography, University of Rhode Island and was partially funded by NSF-OCE 0726543 to B.N.P. This is SOEST contribution number 8153.

## References

- Altabet, M. A. (2007), Constraints on oceanic N balance/imbalance from sedimentary  $^{15}\text{N}$  records, *Biogeosciences*, 4(1), 75–86, doi:10.5194/bg-4-75-2007.
- Altabet, M. A., et al. (1999), The nitrogen isotope biogeochemistry of sinking particles from the margin of the Eastern North Pacific, *Deep Sea Res., Part I*, 46(4), 655–679, doi:10.1016/S0967-0637(98)00084-3.
- Badan-Dangon, A., et al. (1991), The lower atmosphere over the Gulf of California, *J. Geophys. Res.*, 96(C9), 16,877–16,896, doi:10.1029/91JC01433.
- Barron, J. A., et al. (2005), Paleooceanographic history of the Guaymas Basin, Gulf of California, during the past 15,000 years based on diatoms, silicoflagellates, and biogenic sediments, *Mar. Micropaleontol.*, 56(3–4), 81–102, doi:10.1016/j.marmicro.2005.04.001.
- Beaufort, L., et al. (2002), MD126/IMAGES VIII MONA cruise report, *OCE/2002/03*, Inst. Polaire Fr. Paul-Émile Victor, *IPEV*.
- Braman, R. S., and S. A. Hendrix (1989), Nanogram nitrite and nitrate determination in environmental and biological materials by vanadium(III) reduction with chemiluminescence detection, *Anal. Chem.*, 61(24), 2715–2718, doi:10.1021/ac00199a007.
- Brandes, J. A., and A. H. Devol (2002), A global marine-fixed nitrogen isotopic budget: Implications for Holocene nitrogen cycling, *Global Biogeochem. Cycles*, 16(4), 1120, doi:10.1029/2001GB001856.
- Brunner, E., et al. (2009), Chitin-based scaffolds are an integral part of the skeleton of the marine demosponge *Ianthella basta*, *J. Struct. Biol.*, 168(3), 539–547.
- Brzezinski, M. A. (1985), The Si:C:N ratio of marine diatoms: Interspecific variability and the effect of some environmental variables, *J. Phycol.*, 21(3), 347–357, doi:10.1111/j.0022-3646.1985.00347.x.
- Calvert, S. E. (1966), Origin of diatom rich varved sediment from the Gulf of California, *J. Geol.*, 74(5), 546–565.
- Cheshire, H., et al. (2005), Late Quaternary climate change record from two long sediment cores from Guaymas Basin, Gulf of California, *J. Quat. Sci.*, 20(5), 457–469, doi:10.1002/jqs.944.
- Codispoti, L. A. (2007), An oceanic fixed nitrogen sink exceeding 400 Tg  $\text{Na}^{-1}$  vs the concept of homeostasis in the fixed-nitrogen inventory, *Biogeosciences*, 4(2), 233–253, doi:10.5194/bg-4-233-2007.
- DeMaster, D. J. (1981), The supply and accumulation of silica in the marine environment, *Geochim. Cosmochim. Acta*, 45, 1715–1732, doi:10.1016/0016-7037(81)90006-5.
- De Pol-Holz, R., et al. (2009), Controls on sedimentary nitrogen isotopes along the Chile margin, *Deep Sea Res., Part II*, 56(16), 1042–1054, doi:10.1016/j.dsr2.2008.09.014.
- Deutsch, C., et al. (2007), Spatial coupling of nitrogen inputs and losses in the ocean, *Nature*, 445(7124), 163–167, doi:10.1038/nature05392.
- DiFiore, P. J., et al. (2006), Nitrogen isotope constraints on subantarctic biogeochemistry, *J. Geophys. Res.*, 111, C08016, doi:10.1029/2005JC003216.
- Gonfiantini, R., et al. (1995), Reference and intercomparison material for stable isotopes light elements, *IAEA-TECDOC 0825*, 1–159 pp., Int. At. Energy Agency, Vienna.
- Granger, J., and D. M. Sigman (2009), Removal of nitrite with sulfamic acid for nitrate N and O isotope analysis with the denitrifier method, *Rapid Commun. Mass Spectrom.*, 23(23), 3753–3762, doi:10.1002/rcm.4307.
- Hasle, G. R. (2001), The marine, planktonic diatom family Thalassionemataceae: Morphology, taxonomy and distribution, *Diatom Res.*, 16(1), 1–82.
- Hasle, G. R., and G. A. Fryxell (1970), Diatoms: Cleaning and mounting for light and electron microscopy, *Trans. Am. Microsc. Soc.*, 89, 469–474, doi:10.2307/3224555.
- Hidalgo-González, R. M., and S. Alvarez-Borrego (2001), Chlorophyll profiles and the water column structure in the Gulf of California, *Oceanol. Acta*, 24(1), 19–28, doi:10.1016/S0399-1784(00)01126-9.
- Horn, M., et al. (2011), Nitrogen isotopic relationship between diatom-bound and bulk organic matter of cultured polar diatoms, *Paleoceanography*, doi:10.1029/2010PA002080, in press.
- Ingalls, A. E., et al. (2010), Tinted windows: The presence of the UV absorbing compounds called mycosporine-like amino acids embedded in the frustules of marine diatoms, *Cosmochim. Geochim. Acta*, 74(1), 104–115.
- Keigwin, L. D. (2002), Late Pleistocene-Holocene paleoceanography and ventilation of the Gulf of California, *J. Oceanogr.*, 58(2), 421–432, doi:10.1023/A:1015830313175.
- Kemp, A. E. S., et al. (2000), The “Fall dump”—A new perspective on the role of a “shade flora” in the annual cycle of diatom production and export flux, *Deep Sea Res., Part II*, 47(9–11), 2129–2154, doi:10.1016/S0967-0645(00)00019-9.
- Kienast, S. S., et al. (2002), Nitrogen isotope and productivity variations along the northeast Pacific margin over the last 120 kyr: Surface and subsurface paleoceanography, *Paleoceanography*, 17(4), 1055, doi:10.1029/2001PA000650.
- Kroger, N., et al. (1999), Polycationic peptides from diatom biosilica that direct silica nanosphere formation, *Science*, 286(5442), 1129–1132.
- Lavin, M. F., and S. G. Marinone (2003), An overview of the physical oceanography of the Gulf of California, in *Nonlinear Processes in Geophysical Fluid Dynamics*, edited by P. Ripa et al., Kluwer Acad., Dordrecht, Netherlands, doi:10.1007/978-94-010-0074-1\_11.
- Liu, K.-K., and I. R. Kaplan (1989), The eastern tropical Pacific as a source of  $^{15}\text{N}$ -enriched nitrate in seawater off southern California, *Limnol. Oceanogr.*, 34, 820–830, doi:10.4319/lo.1989.34.5.0820.
- Mortlock, R. A., and P. N. Froelich (1989), A simple method for the rapid determination of biogenic opal in pelagic marine sediments, *Deep Sea Res., Part I*, 36, 1415–1426, doi:10.1016/0198-0149(89)90092-7.
- Needoba, J. A., and P. J. Harrison (2004), Influence of low light and a light: Dark cycle on  $\text{NO}_3^-$  uptake, intracellular  $\text{NO}_3^-$ , and nitrogen isotope fractionation by marine phytoplankton, *J. Phycol.*, 40(3), 505–516, doi:10.1111/j.1529-8817.2004.03171.x.

- Pike, J., and A. E. S. Kemp (1997), Early Holocene decadal-scale ocean variability recorded in Gulf of California laminated sediments, *Paleoceanography*, *12*(2), 227–238, doi:10.1029/96PA03132.
- Pride, C., et al. (1999), Nitrogen isotopic variations in the Gulf of California since the last deglaciation: Response to global climate change, *Paleoceanography*, *14*(3), 397–409, doi:10.1029/1999PA900004.
- Robinson, R. S., and D. M. Sigman (2008), Nitrogen isotopic evidence for a poleward decrease in surface nitrate within the ice age Antarctic, *Quat. Sci. Rev.*, *27*(9–10), 1076–1090, doi:10.1016/j.quascirev.2008.02.005.
- Robinson, R. S., et al. (2004), Revisiting nutrient utilization in the glacial Antarctic: Evidence from a new method for diatom-bound N isotopic analysis, *Paleoceanography*, *19*, PA3001, doi:10.1029/2003PA000996.
- Robinson, R. S., et al. (2005), Diatom-bound <sup>15</sup>N/<sup>14</sup>N: New support for enhanced nutrient consumption in the ice age subantarctic, *Paleoceanography*, *20*, PA3003, doi:10.1029/2004PA001114.
- Sancetta, C. (1995), Diatoms in the Gulf of California: Seasonal flux patterns and the sediment record for the last 15,000 years, *Paleoceanography*, *10*(1), 67–84, doi:10.1029/94PA02796.
- Sancetta, C., et al. (1991), Massive fluxes of rhizosolenid diatoms: A common occurrence?, *Limnol. Oceanogr.*, *36*(7), 1452–1457, doi:10.4319/lo.1991.36.7.1452.
- Scheffel, A., et al. (2011), Nanopatterned protein microrings from a diatom that direct silica morphogenesis, *Proc. Natl. Acad. Sci. U. S. A.*, *108*(8), 3175–3180.
- Shemesh, A., et al. (1993), Isotopic evidence for reduced productivity in the glacial Southern Ocean, *Science*, *262*(5132), 407–410, doi:10.1126/science.262.5132.407.
- Shimada, C., et al. (2008), Paleoecological significance of laminated diatomaceous oozes during the middle-to-late Pleistocene, North Atlantic Ocean (IODP Site U1304), *Mar. Micropaleontol.*, *69*(2), 139–150, doi:10.1016/j.marmicro.2008.07.004.
- Sigman, D. M., et al. (1999), The  $\delta^{15}\text{N}$  of nitrate in the southern ocean: Consumption of nitrate in surface waters, *Global Biogeochem. Cycles*, *13*(4), 1149–1166, doi:10.1029/1999GB900038.
- Sigman, D. M., et al. (2001), A bacterial method for the nitrogen isotopic analysis of nitrate in seawater and freshwater, *Anal. Chem.*, *73*(17), 4145–4153, doi:10.1021/ac010088e.
- Thunell, R. C. (1998), Seasonal and annual variability in particle fluxes in the Gulf of California: A response to climate forcing, *Deep Sea Res., Part I*, *45*(12), 2059–2083, doi:10.1016/S0967-0637(98)00053-3.
- Verardo, D. J., et al. (1990), Determination of organic carbon and nitrogen in marine sediments using the Carlo Erba NA-1500 analyzer, *Deep-Sea Res., Part A*, *37*(1), 157–165.
- Wada, E., and A. Hattori (1976), Natural abundance of <sup>15</sup>N in particulate organic matter in the North Pacific Ocean, *Geochim. Cosmochim. Acta*, *40*, 249–251.
- White, A. E., et al. (2007), Summer surface waters in the Gulf of California: Prime habitat for biological N<sub>2</sub> fixation, *Global Biogeochem. Cycles*, *21*, GB2017, doi:10.1029/2006GB002779.